J Mol Hist (2014) 45:121–128
DOI 10.1007/s10735-013-9537-0

SHORT COMMUNICATION

A novel adenoviral vector-mediated mouse model of Charcot-Marie-Tooth type 2D (CMT2D)

Ah Jung Seo · Youn Ho Shin · Seo Jin Lee · Doyeun Kim · Byung Sun Park · Sunghoon Kim · Kyu Ha Choi · Na Young Jeong · Chan Park · Ji-Yeon Jang · Youngbuhm Huh · Junyang Jung

Received: 26 June 2013 / Accepted: 23 August 2013 / Published online: 30 August 2013

Abstract Charcot-Marie-Tooth disease type 2D is a hereditary axonal and glycyl-tRNA synthetase (GARS)-associated neuropathy that is caused by a mutation in GARS. Here, we report a novel GARS-associated mouse neuropathy model using an adenoviral vector system that contains a neuronal-specific promoter. In this model, we found that wild-type GARS is distributed to peripheral axons, dorsal root ganglion (DRG) cell bodies, central axon terminals, and motor neuron cell bodies. In contrast, GARS containing a G240R mutation was localized in DRG and motor neuron cell bodies, but not axonal regions, in vivo. Thus, our data suggest that the disease-causing G240R mutation may result in a distribution defect of GARS in peripheral nerves in vivo. Furthermore, a distributional defect may be associated with axonal degradation in GARS-associated neuropathies.

Ah Jung Seo and Youn Ho Shin have contributed equally to this work.

A. J. Seo · Y. H. Shin · S. J. Lee · B. S. Park · K. H. Choi · C. Park · J.-Y. Jang · Y. Huh (✉) · J. Jung (✉)
Department of Anatomy and Neurobiology, School of Medicine, Kyung Hee University, Heogi-Dong 1, Dongdaemun-Gu, Seoul 130-701, Republic of Korea
e-mail: ybhuh@khu.ac.kr

J. Jung
e-mail: jjung@khu.ac.kr

D. Kim · S. Kim
Medicinal Bioconvergence Research Center, Seoul National University, Seoul 151-742, Republic of Korea

N. Y. Jeong
Department of Anatomy and Cell Biology and Mitochondria, Hub Regulation Center, Dong-A University College of Medicine, 3-1 Dongdaesin-dong, Seo-gu, Busan 602-714, Republic of Korea

Keywords Charcot-Marie-Tooth disease · Axonal degeneration · Recombinant adenovirus · Glycyl-tRNA synthetase · Demyelination

Introduction

Glycyl-tRNA synthetase (GARS), a member of the family of aminoacyl-tRNA synthetases, is ubiquitously expressed in both neuronal and non-neuronal cells. Because these enzymes are essential for translation during protein synthesis in living cells, the mutation and dysregulation of GARS protein has been implicated in the pathogenesis of several human diseases (Ge et al. 1994; Sivakumar et al. 2005). Charcot-Marie-Tooth disease (CMT) is a commonly inherited peripheral neuropathy. A G240R mutation in the GARS gene has been linked to Charcot-Marie-Tooth disease type 2D (CMT2D), which is an axonal neuropathy characterized by impaired motor function and sensory loss in the extremities (Antonellis et al. 2003).

Two studies examined the localization of wild type (WT) and G240R mutant GARS in a cell culture system (Antonellis et al. 2006; Nangle et al. 2007). Antonellis et al. found that WT GARS protein existed in a granular form within the cell body and neurite projections, whereas the G240R mutant was diffusely distributed throughout the whole cell and was not granular (Antonellis et al. 2006). In contrast, another study suggested that WT GARS showed a diffuse pattern in neuroblastoma cells, whereas the G240R mutant was present at lower levels and in neurite projections (Nangle et al. 2007). Motley et al. created a mouse model containing a mouse-specific mutation that creates the CMT phenotype. They then used this model to investigate the localization of the mouse GARS protein (Motley et al. 2011). However, although studies have been carried

out using this model (Motley et al. 2011; Stum et al. 2011), there is still no clear in vivo evidence to confirm the localization of the human mutant GARS protein that induces CMT2D in human peripheral nerves.

To confirm the effects of G240R mutant GARS in CMT2D, we constructed in vivo mouse models using neuron-specific adenoviral vectors and examined the localization of WT and G240R mutant GARS proteins in peripheral nerves. We employed an adenovirus vector system containing a neuronal-specific promoter to achieve strong transgene expression exclusively in neurons in vivo. Our data suggest that the distribution defect of the GARS mutant may explain the CMT2D phenotype.

Materials and methods

Animals

All experiments were performed on 6-week-old male C57BL/6 mice. Mice were housed in a temperature- and humidity-controlled environment on a 12-h light/dark cycle with free access to food and water, and cages were changed weekly. All animal procedures were performed in accordance with guidelines of the Korean Academy of Medical Science and were approved by the Kyung Hee University Committee on Animal Research. Every effort was made to minimize the number of animals used and the suffering of the animals.

Neuronal-specific recombinant adenoviruses

The mouse choline acetyltransferase (ChAT) promoter (GenBank accession number NC_000080), which contains key regulatory elements for neuron-specific expression, including a neuron-restrictive silencer element (NRSE) and a cholinergic-specific enhancer (Misawa et al. 1992; Lönnerberg et al. 1996), was used. Human GARS (hGARS) clones were used to allow sub-cloning into the pAdTrack-ChAT-CMV/GFP vector. An E1/E3 double-deletion supercoiled adenoviral backbone vector (pAdEasy-1; Stratagene, Santa Clara, CA, USA) was then used to generate stable homologous recombinants of FLAG-tagged pAdTrack-ChAT-hGARS^{wt}-CMV/GFP and pAdTrack-ChAT-hGARS^{G240R}-CMV/GFP (Fig. 1a). Recombinant adenoviruses in AD293 cells were concentrated and purified using density gradient separation with cesium chloride ($CsCl_2$), followed by ultracentrifugation. Finally, concentrated viruses in $CsCl_2$ were transferred to an optimum buffer (10 mM Tris–Cl pH 8.0, 2 mM $MgCl_2$, 5 % sucrose) by membrane dialysis (Spectrum Laboratories, Rancho Dominquez, CA, USA). Titration of recombinant adenoviruses was then performed by the cytopathic effect method (Nyberg-Hoffman et al. 1997). The titers of Ad*h*GARS^{WT}/ChAT and Ad*h*GARS^{G240R}/ChAT used in these experiments were 5.1×10^9 (pfu/ml) and 2.6×10^9 (pfu/ml), respectively.

Viral administration

Recombinant adenoviruses were injected into the sciatic nerve for anterograde and retrograde transduction. Mice were anesthetized with 30-mg/kg Zoletil (Virbac, Carros Sedecs, France) and 10-mg/kg Rompun (Bayer, Leverkusen, Germany), and the sciatic nerve was surgically exposed by incision of the musculus gluteus superficialis. The nerve was gently placed onto forceps, and viral diluents containing 1.5 µl Ad*h*GARS^{WT}/ChAT or 3 µl Ad*h*GARS^{G240R}/ChAT were injected, along with Fast Green (Sigma, St. Louis, MO, USA) to visualize the viral infusion. The injections were performed with a fine capillary microinjection needle, which was extracted using a Narishige puller (PC-10) attached to a 25-µl Hamilton syringe via rubber tubing to minimize nerve insult. The skin incision was then closed with sutures (B/Braun, Melsungen, Germany, Silkam 4.0).

Tissue processing

Seven days after administration of the virus, the sciatic nerve, the L4/L5 dorsal root ganglia, and the spinal cord were collected and stored as appropriate for each experiment. For immunohistochemistry (IHC), tissues were perfused with 4 % paraformaldehyde (PFA) in 0.1 M phosphate buffer (PB) and then dissected. The samples were immersed in the same solution overnight at 4 °C, followed by incubation in 30 % sucrose in 0.1-M PB for 3 days. They were then embedded in OCT and frozen immediately on dry ice. Frozen sections (16 µm) were cut from tissues and mounted on slides (Fisher Scientific, Houston, TX, USA).

For the analysis of protein and RNA, the sciatic nerve, L4/L5 the dorsal root ganglia, and the spinal cord were isolated from animals immediately after sacrifice by CO_2 inhalation. Sciatic nerve sheaths were removed in ice-cold PBS, and the spinal cord was separated into the dorsal and ventral horns at the L4–L6 segment. Protein lysates were then prepared as follows: tissues were homogenized in a modified radioimmunoprecipitation assay buffer (RIPA; 50 mmol/L Tris–HCl pH 7.4, 150 mmol/L NaCl, 0.5 % deoxycholic acid, 0.5 % Triton X-100, 1 mmol/L phenylmethylsulfonyl fluoride, 1 mmol/L sodium *o*-vanadate, and protease inhibitor cocktail [Roche Molecular Biochemicals, Nutley, NJ, USA]). Lysates were centrifuged at 14,000×*g* for 15 min at 4 °C, and supernatants were collected. Protein concentrations were quantified using a Bradford assay following standard protocols.

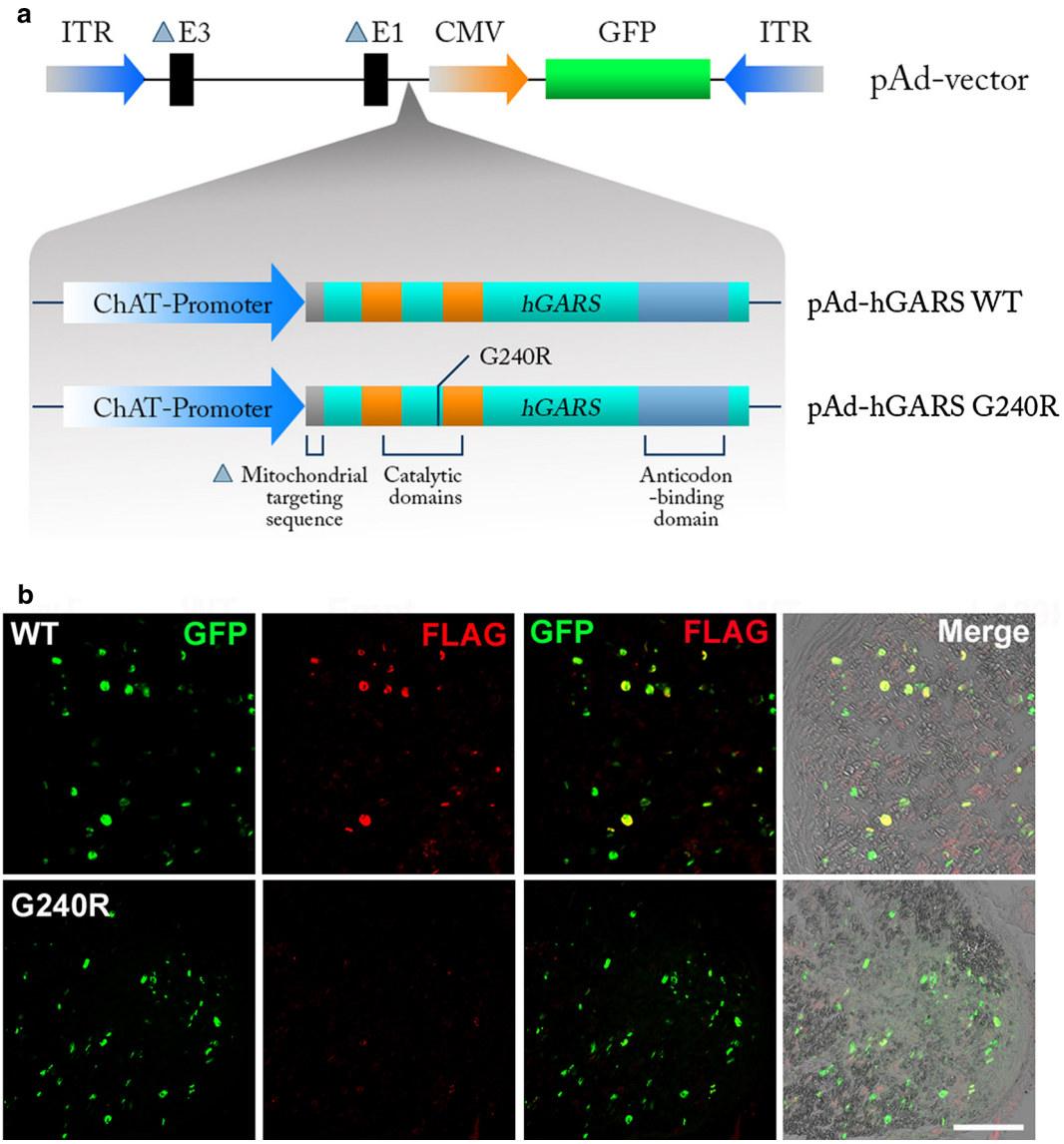

Fig. 1 Neuronal-specific expression of human GARS proteins in sciatic nerves. **a** Schematic representation of the promoter and expression units of each adenovirus construct (GARS WT and G240R). The mitochondrial targeting sequence was deleted to prevent GARS proteins from being expressed in mitochondria. **b** Neuronal-specific expression of GARS (hGARS) proteins in sciatic nerves. GFP expression (*green*) and immunofluorescence labeling of FLAG (*red*) are shown in cross-sections of the sciatic nerve, whereas *yellow staining* indicates an overlap of the *green and red signals*. *GFP-FLAG* double-staining indicates the expression of FLAG-tagged hGARS fusion proteins. *Scale bar* 20 μm. (Color figure online)

Immunofluorescence labeling

Before staining, slides were fixed in 4 % PFA for 10 min. After 3 washes with phosphate-buffered saline (PBS), the samples were permeabilized in PBS containing 0.3 % Triton X-100 (PBST) and blocked with 10 % bovine serum albumin (BSA) overnight at 4 °C. Rabbit anti-FLAG (1:500; Cell Signaling Technology, Danvers, MA, USA) primary antibody was placed on the slides, which were incubated for 1 h. After three washes with PBS, samples were incubated for 2 h with Alexa Fluor 594 donkey anti-rabbit secondary antibody. The slides were then washed with PBS and mounted. The immunofluorescence was detected and analyzed using a laser scanning confocal microscope (LSM700, Carl Zeiss, Oberkochen, Germany). All incubations were carried out at room temperature unless otherwise indicated.

Nerve fiber teasing

After perfusion with 4 % PFA, sciatic nerves were detached and incubated for 24 h in 4 % paraformaldehyde, followed by PBS for 24 h at 4 °C. Nerves were then transferred to ice-cold PBS for dissection and teasing.

Nerves were cut into small segments 5 mm in length under a stereoscope after the nerve sheath had been removed. Nerve segments were then separated using micro-fine forceps and straightened on to the slides. The slides were dried for 1 h at room temperature, and immunofluorescence staining was performed, as described above, using goat anti-P0 (1:1,000; Santa Cruz Biotechnology, Dallas, TX, USA) and Alexa Fluor 594 donkey anti-goat (Invitrogen, Carlsbad, CA, USA) antibodies.

Western blotting

Protein extracts were separated by 10 % sodium dodecyl sulfate polyacrylamide gel electrophoresis and transferred to nitrocellulose membranes. To prevent non-specific binding, membranes were blocked overnight in 5 % non-fat milk in Tris-buffered saline (TBS) containing 0.05 % Tween-20 (TBST). The membranes were then incubated with either mouse anti-β-actin (1:5,000; Sigma, St. Louis, MO, USA) or rabbit anti-FLAG (1:1,000; Cell Signaling Technology, Danvers, MA, USA) primary antibodies for 1 h at room temperature. After three washes in TBST, the blots were incubated with the appropriate horseradish peroxidase-conjugated secondary antibodies. After three additional washes in TBST, membranes were developed using an enhanced chemiluminescence system (Amersham, Buckinghamshire, England). All experiments were repeated at least three times.

Statistical analysis

Differences in the means between groups were statistically analyzed using analysis of variance followed by Bonferroni's post hoc test. Differences were considered to be statistically significant at $p < 0.01$ after the analysis of three independent experiments.

Results and discussion

Previous studies revealed that the G240R mutant protein plays a role in the pathogenesis of Charcot-Marie-Tooth type 2D (CMT2D) (Antonellis et al. 2003; Ionasescu et al. 1996; Christodoulou et al. 1995). To assess CMT2D in vivo, we employed an adenovirus vector system using the pAdeasy-ChAT-hGARS-Flag-CMV-GFP that expresses the FLAG-tagged human GARS under the control of the neuronal-specific choline acetyltransferase (ChAT) promoter and the GFP under the control of a CMV promoter. These vectors were then injected into the sciatic nerves of mice to create WT and G240R hGARS-overexpressing mouse models (Fig. 1a). We then used IHC with an anti-FLAG antibody to detect the expression of infected WT and G240R GARS genes in the sciatic nerve. Because the expressed GFP is translated from a distinct transcript driven by a CMV promoter, all vectors (WT and G240R) exhibited GFP-positive signals (Fig. 1b). These findings therefore suggest the operation of neuronal-specific expression of FLAG-tagged hGARS fusion proteins in the peripheral axons.

In a previous study analyzing the cellular localization of hGARS variants in vitro, immunofluorescence showed that WT hGARS is diffusely localized in N2a neuronal cells, but that the G240R mutant is expressed at lower levels and in the neurite projections (Nangle et al. 2007). To assess differences in the in vivo distribution of WT and G240R mutant GARS proteins in peripheral nerves, we analyzed sciatic nerve fibers infected with WT and G240R mutant hGARS-producing adenoviruses. Immunofluorescence using an anti-FLAG antibody, which detected the infected WT and G240R mutant hGARS proteins, showed clear staining along the length of the axons in WT hGARS-expressing sciatic nerve fibers 7 days after adenoviral infection (Fig. 2a, b). In contrast, the G240R hGARS mutant protein was not localized in the axons of sciatic nerve fibers (Fig. 2a, b). Additionally, the patterns of anti-FLAG staining in nerve cross-sections were also different between groups, and the GARS mutant-expressing sciatic nerves did not express the GARS-FLAG fusion protein as efficiently as it expressed WT (Fig. 1b). To confirm these observations, we also performed western blotting using an anti-FLAG antibody to assess the relative expression of the hGARS proteins in sciatic nerve fibers and found that the G240R mutant hGARS protein was expressed at lower levels than was the WT protein (Fig. 2c, d).

The afferent fibers of the sensory neurons, whose cell bodies lie in the DRG, terminate in projection neurons in the dorsal horn of the spinal cord. Differences in the expression of WT and G240R hGARS proteins in this region may also be relevant for identifying the primary cause of CMT2D. We therefore carried out western blotting using total protein samples from the dorsal horn of the spinal cord isolated 7 days after adenoviral infection. The data revealed that the G240R mutant hGARS protein was expressed at lower levels than was the WT protein in the dorsal horn of the spinal cord, which is consistent with observations in the sciatic nerve (Fig. 3c, d).

The ventral horn of the spinal cord contains motor neurons, and their axons stretch from the central cell bodies to peripheral nerves to affect the axial muscles. To identify the distribution pattern of WT and G240R mutant hGARS in the axons of motor neurons, we carried out immunofluorescence staining for FLAG-tagged hGARS on adenovirus-infected spinal cords 7 days after infection and found that both proteins were expressed in motor-neuronal cell bodies (Fig. 3a). These findings were confirmed by western

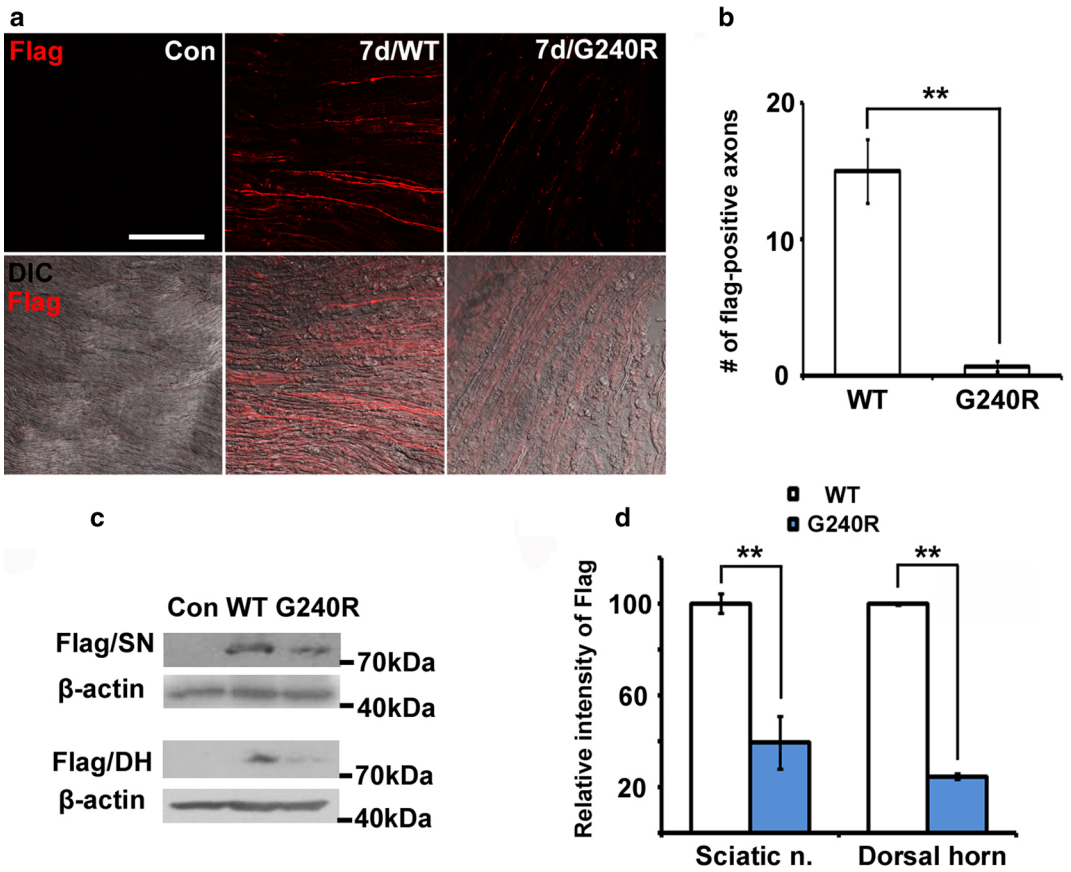

Fig. 2 Distribution patterns of hGARS proteins in peripheral axons. **a** The distribution defect of G240R mutant hGARS in sciatic nerve fibers. The intensity of FLAG staining (*red*) was decreased in G240R mutant-expressing samples compared with WT samples in sciatic nerve cross-sections. *Scale bar* 100 μm. **b** Flag-positive axons were counted in 300-μm spaced cross-sections. A total of nine sections from three animals were used for quantification ($n = 5$ mice per group; $^{**}P < 0.01$). **c** Protein lysates from adenovirus-infected mouse sciatic nerves (SN) and spinal dorsal horns (DH) were analyzed by western blotting, *Con* control. **d** Quantification of western blotting was used to calculate the relative intensity of the FLAG bands. FLAG expression was decreased in G240R-mutant hGARS-expressing sciatic nerves and spinal dorsal horn samples compared with WT expression ($n = 4$–5 mice; $^{**}P < 0.01$). (Color figure online)

blotting, which identified expression of WT and G240R mutant hGARS motor neurons of the spinal ventral horn (Fig. 3c, d).

Next, we analyzed the expression of WT and G240R mutant hGARS in sensory neuronal cell bodies using the adenovirus-infected mouse model. A previous study found that ChAT could be visualized by IHC in DRG neurons (Bellier and Kimura 2007). To identify the expression of WT and G240R mutant hGARS in the dorsal root ganglion (DRG) after adenoviral infection, we assessed the expression of FLAG-tagged hGARS by immunofluorescence staining in DRG samples 7 days after adenoviral infection. In both WT and G240R mutant hGARS-expressing DRG, FLAG-positive signals co-localized with GFP fluorescence (Fig. 3b). Western blotting followed by quantitation then confirmed that WT and G240R hGARS mutant proteins were expressed at similar levels in DRG neuronal cell bodies (Fig. 3b, d).

Patients with CMT2D have normal motor nerve conduction velocity and no demyelination in axonal neuropathy (Hamaguchi et al. 2010). To confirm the in vivo differences in myelination of the sciatic nerve fibers in mice infected with WT and G240R mutant hGARS, we assessed myelination by immunofluorescence using a P0 antibody as a marker of the myelin sheath. We compared the intensity of P0 fluorescence staining in GFP-positive teased axons between WT and G240R mutant-expressing neurons and found that the relative intensity of P0 was comparable between the two groups (Fig. 4a). Although the relative number of intact P0-positive sciatic nerve fibers to GFP-positive axons was comparable between the two groups, only a limited number of GFP-positive axons were observed due to the distribution defect of the G240R mutant (Fig. 4b). These observations were confirmed by western blotting, where visual inspection and quantitative analysis revealed similar expression of the myelin-associated proteins P0 in WT and G240R mutant hGARS-expressing sciatic nerves (Fig. 4c, d).

Previous studies assessed the distribution patterns of the disease-causing G240R mutant hGARS protein in an in vitro

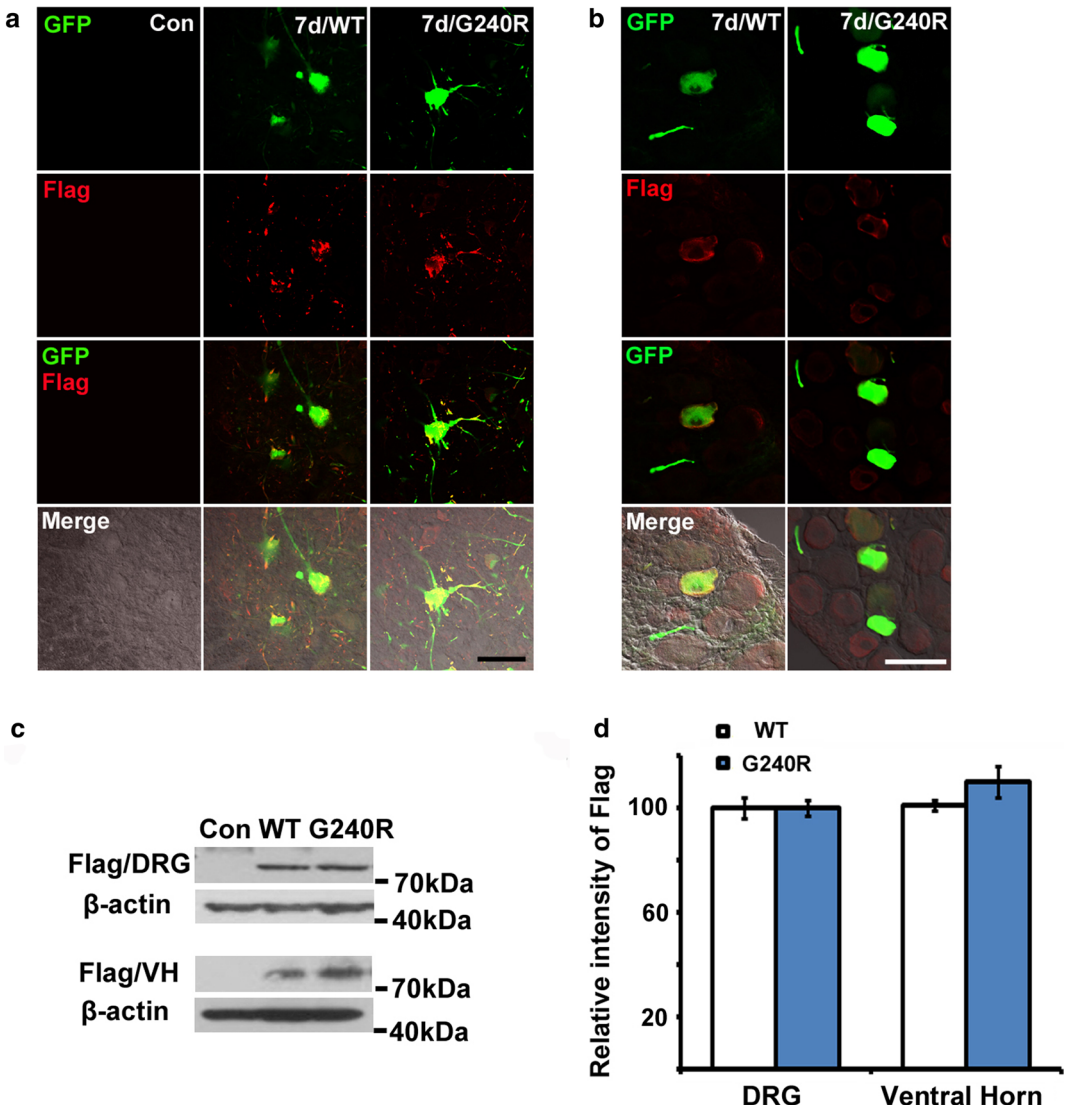

Fig. 3 Distribution patterns of hGARS proteins in the cell bodies of sensory and motor neurons. **a** The expression of FLAG-tagged hGARS fusion proteins in motor-neuronal cell bodies of the spinal ventral horn. Confocal images show the expression of GFP (*green*) and FLAG (*red*) using immunofluorescence labeling in spinal cord cross-sections. *Scale bar* 100 μm. **b** Expression of FLAG-tagged hGARS fusion proteins in the cell bodies of dorsal root ganglia (DRG). Immunofluorescent analysis of GFP (*green*) and FLAG (*red*) expression in the DRG are shown. *Scale bar* 50 μm. **c** Protein lysates from mouse DRG or spinal ventral horn after adenoviral infection were analyzed using western blotting. *WT* wild type, *G240R* G240R mutant hGARS. **d** Quantification of western blotting showed the relative intensity of the FLAG bands. In the DRG, equal expression of the hGARS proteins was observed. In contrast, the expression of the G240R mutant was decreased compared with that of WT hGARS in the ventral horn ($n = 4$–5 mice). (Color figure online)

system. Antonellis et al. used enhanced green fluorescent protein-tagged WT or mutant hGARS in MN-1 cells and found that WT hGARS associates with cytoplasmic granules, whereas G240R mutant hGARS is not associated with a granular form and is distributed diffusely throughout the entire cell (Antonellis et al. 2006). In contrast, another study using in vitro immunostaining of V5 epitope-tagged WT or mutant hGARS revealed low expression and altered localization of the mutant hGARS to N2a neurite projections, whereas WT was diffusely localized (Nangle et al. 2007). These discrepancies therefore needed to be resolved in vivo, using an animal model suitable for identifying the localization of WT and G240R mutant hGARS proteins. We therefore produced a CMT2D mouse model that could be used to identify the distribution of WT or G240R mutant proteins in sciatic nerves, the DRG, the spinal dorsal horn, and the spinal ventral horn using FLAG-tagged hGARS fusion-expressing adenoviruses (Figs. 2, 3). However, it is feasible that the lack of G240R GARS detected in axons may be due to the degeneration of G240R-infected neurons. There are therefore two possibilities: (1) axonal-degeneration-induced loss of G240R GARS expression in axons; and (2)

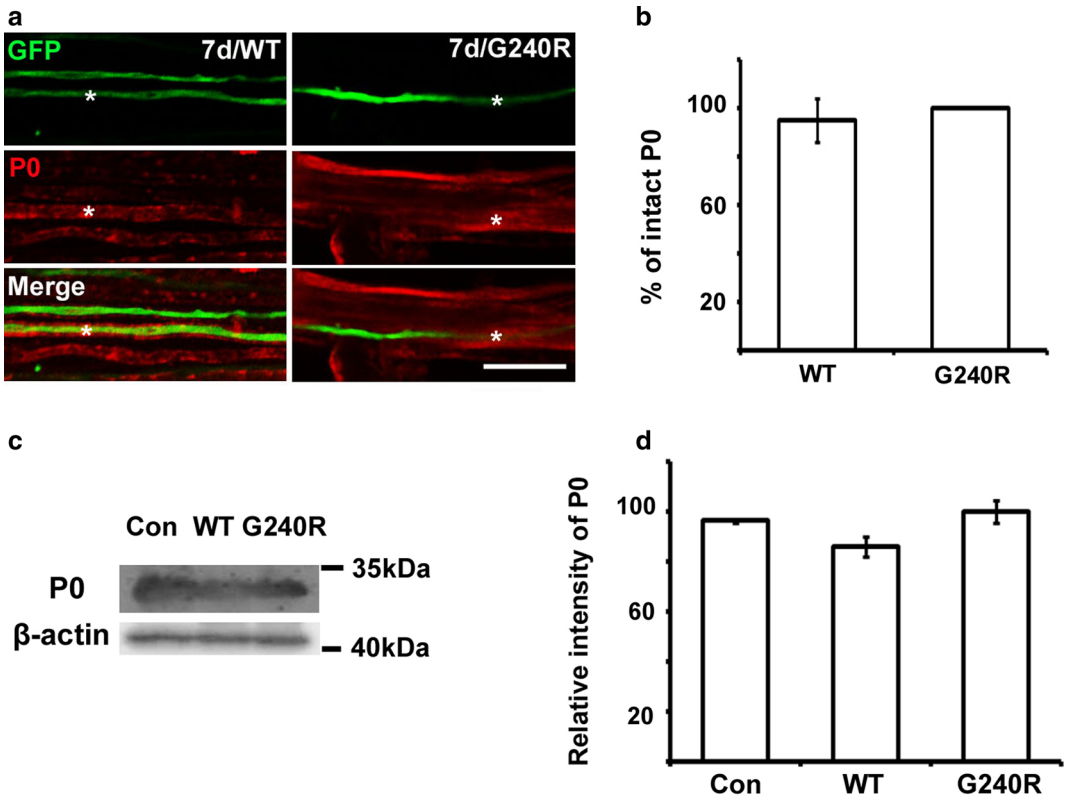

Fig. 4 Conservation of myelin sheaths in the CMT2D mouse model. **a** No difference in the levels of myelin sheath was detected between WT and G240R mutant hGARS-expressing myelinating sciatic nerve fibers. Confocal images show GFP expression (*green*) and immunofluorescence labeling of protein zero (P0, *red*, a marker for myelin sheaths) in the teased sciatic nerve fibers (denoted by *asterisks*). *Scale bar* 20 μm. **b** Percentage of intact P0-positive nerve fibers from WT and G240R mutants. **c** Protein lysates from mouse sciatic nerves from adenovirally-infected mice were analyzed by western blotting ($n = 5$ mice). **d** Quantitation of western blotting revealed the relative intensity of the P0 bands. No significant differences were observed in the myelin sheath between WT and G240R mutant hGARS-expressing nerve fibers ($n = 5$ mice). (Color figure online)

axonal degeneration due to the lack of G240R GARS in axons. However, we cannot yet distinguish which of these occurs. Because one of the phenotypes in CMT2D is axonal degeneration, assessing this process with mutant GARS in our model may help explain the phenotypes of CMT2D.

Our adenovirus mouse model showed that the myelin sheath is conserved in both WT and G240R mutant hGARS-expressing sciatic nerves (Fig. 4). Although western blotting data showed lower levels of the myelin sheath protein P0 in adenovirus-infected sciatic nerves compared with non-infected controls, there was little difference in the expression of P0 between the sciatic nerve fibers expressing WT or G240R mutant proteins (Fig. 4c, d). This model may therefore be a useful tool for studying the phenotypes of CMT2D.

In conclusion, we identified distributional differences between WT and G240R mutant GARS proteins in long axons using an in vivo animal model. Several studies have suggested that the loss of charging function is a possible mechanism for GARS axonopathy (Motley et al. 2010; Antonellis and Green 2008). However, even though there is no loss of function of the GARS G240R mutant in vivo, the distribution defect may have an adverse effect on the axon terminals of long-distance-peripheral nerves. Additional studies are therefore needed to identify the cause of the distribution defect of the mutant GARS protein. Thus, the findings of this study may be useful for understanding the pathophysiology of CMT2D and provide a potential target for developing therapeutic interventions for CMT2D.

Acknowledgments We thank Dr. Paul Schimmel (Scripps Research Institute; La Jolla, CA) for kindly providing the WT and G240R mutant GARS clones. This work was supported by a Global Frontier Project Grant (2012M3A6A2011-0032149) from the National Research Foundation funded by the Ministry of Education, Science and Technology of Korea and a National Research Foundation of Korea (NRF) Grant funded by the Korean government (MEST; No. 20120009380).

References

Antonellis A, Green ED (2008) The role of aminoacyl-tRNA synthetases in genetic diseases. Annu Rev Genomics Hum Genet 9:87–107

Antonellis A, Ellsworth RE, Sambuughin N, Puls I, Abel A, Lee-Lin SQ, Jordanova A, Kremensky I, Christodoulou K, Middleton LT, Sivakumar K, Ionasescu V, Funalot B, Vance JM, Goldfarb LG, Fischbeck KH, Green ED (2003) Glycyl tRNA synthetase mutations in Charcot-Marie-Tooth disease type 2D and distal spinal muscular atrophy type V. Am J Hum Genet 72:1293–1299

Antonellis A, Lee-Lin SQ, Wasterlain A, Leo P, Quezado M, Goldfarb LG, Myung K, Burgess S, Fischbeck KH, Green ED (2006) Functional analyses of glycyl-tRNA synthetase mutations suggest a key role for tRNA-charging enzymes in peripheral axons. J Neurosci 26:10397–10406

Bellier JP, Kimura H (2007) Acetylcholine synthesis by choline acetyltransferase of a peripheral type as demonstrated in adult rat dorsal root ganglion. J Neurochem 101:1607–1618

Christodoulou K, Kyriakides T, Hristova AH, Georgiou DM, Kalaydjieva L, Yshpekova B, Ivanova T, Weber JL, Middleton LT (1995) Mapping of a distal form of spinal muscular atrophy with upper limb predominance to chromosome 7p. Hum Mol Genet 4:1629–1632

Ge Q, Trieu EP, Targoff IN (1994) Primary structure and functional expression of human Glycyl-tRNA synthetase, an autoantigen in myositis. J Biol Chem 269:28790–28797

Hamaguchi A, Ishida C, Iwasa K, Abe A, Yamada M (2010) Charcot-Marie-Tooth disease type 2D with a novel glycyl-tRNA synthetase gene (GARS) mutation. J Neurol 257:1202–1204

Ionasescu V, Searby C, Sheffield VC, Roklina T, Nishimura D, Ionasescu R (1996) Autosomal dominant Charcot-Marie-Tooth axonal neuropathy mapped on chromosome 7p (CMT2D). Hum Mol Genet 5:1373–1375

Lönnerberg P, Schoenherr CJ, Anderson DJ, Ibáñez CF (1996) Cell type-specific regulation of choline acetyltransferase gene expression. Role of the neuron-restrictive silencer element and cholinergic-specific enhancer sequences. J Biol Chem 271: 33358–33365

Misawa H, Ishii K, Deguchi T (1992) Gene expression of mouse choline acetyltransferase. Alternative splicing and identification of a highly active promoter region. J Biol Chem 267:20392–20399

Motley WW, Talbot K, Fischbeck KH (2010) GARS axonopathy: not every neuron's cup of tRNA. Trends Neurosci 33:59–66

Motley WW, Seburn KL, Nawaz MH, Miers KE, Cheng J, Antonellis A, Green ED, Talbot K, Yang XL, Fischbeck KH, Burgess RW (2011) Charcot-Marie-Tooth-linked mutant GARS is toxic to peripheral neurons independent of wild-type GARS levels. PLoS Genet 7:e1002399

Nangle LA, Zhang W, Xie W, Yang XL, Schimmel P (2007) Charcot-Marie-Tooth disease-associated mutant tRNA synthetases linked to altered dimer interface and neurite distribution defect. Proc Natl Acad Sci USA 104:11239–11244

Nyberg-Hoffman C, Shabram P, Li W, Giroux D, Aguilar-Cordova E (1997) Sensitivity and reproducibility in adenoviral infectious titer determination. Nat Med 3:808–811

Sivakumar K, Kyriakides T, Puls I, Nicholson GA, Funalot B, Antonellis A, Sambuughin N, Christodoulou K, Beggs JL, Zamba-Papanicolaou E, Ionasescu V, Dalakas MC, Green ED, Fischbeck KH, Goldfarb LG (2005) Phenotypic spectrum of disorders associated with glycyl-tRNA synthetase mutations. Brain 128:2304–2314

Stum M, McLaughlin HM, Kleinbrink EL, Miers KE, Ackerman SL, Seburn KL, Antonellis A, Burgess RW (2011) An assessment of mechanisms underlying peripheral axonal degeneration caused by aminoacyl-tRNA synthetase mutations. Mol Cell Neurosci 46:432–443